Supplement to

The Ability of Hydrologic-Land Surface Models to Concurrently Simulate Permafrost and Hydrology

Mohamed S. Abdelhamed, Mohamed E. Elshamy, Saman Razavi, Howard S. Wheater

S1. Model configuration

The soil column discretization for all configurations was implemented using a power-function approach (**Table S1**), with a total depth of 51.24 m and a fine layering for the upper 2 m of the soil (9 layers), in line with ground observations and gridded products for active layer thickness (ALT). Noting that the double-precision computations (of MESH model) were employed to resolve the tiny changes in temperature and heat fluxes, as recommended by Harvey and Verseghy (2016) for deep soil columns (>25m).

Table S1. Soil profile layering scheme for the two sites (adopted form (Elshamy et al., 2020)).

Layer	Thickness	Layer	Thickness
1	0.10	14	1.48
2	0.11	15	1.78
3	0.12	16	2.11
4	0.14	17	2.48
5	0.17	18	2.88
6	0.21	19	3.33
7	0.27	20	3.81
8	0.35	21	4.34
9	0.47	22	4.90
10	0.63	23	5.51
11	0.80	24	6.17
12	0.99	25	6.87
13	1.22		

The Canada Centre for Remote Sensing (CCRS) 2005 dataset (Canada Centre for Remote Sensing et al., 2010) was used to parameterize land cover classes into different group response unit (GRU), as summarized in **Table S2**.

Table S2. List of model GRUs and the associated fractional coverage over the LRB.

No.	GRU	Area (%)
1	Urban	0.001
2	Barrenland	7.864
3	Snow/Ice	0.414
4	Lichen-Moss	3.024
5	Water	1.411
6	Grass	2.389
7	Cropland	0.001
8	Wetland	3.611
9	Shrubs	9.482
10	Needleleaf Forest	52.698
11	Mixed/Broadleaf Forest	19.105

The depth of organic soil (ODEP) was configured as either a fixed depth (top six layers, 0.85 m) or a varying depth (spatially) following the linear relationship between ODEP and the soil organic content (**Fig. S1**). The peat depth was extracted from several Geological Survey of Canada reports for 75 boreholes covering the Mackenzie River Basin domain (**Table S3**), and the corresponding soil organic content (as a percentage) was derived from Soil Landscapes of Canada (SLC) v2.2 (Centre for Land and Biological Resources Research, 1996), as shown in **Fig. 1E** in the main text.
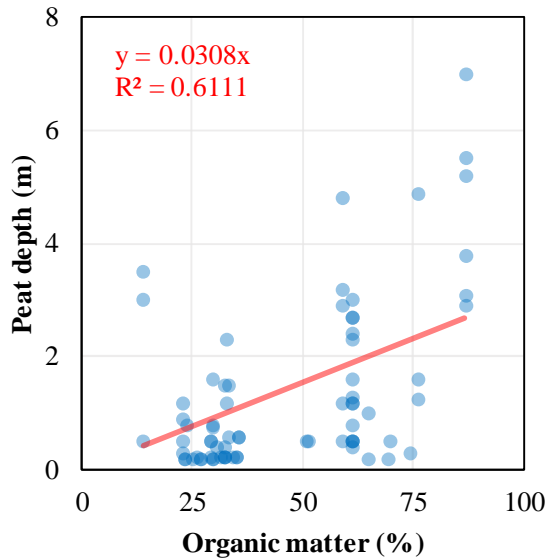
Fig. S1. The relationship between peat depth and organic matter extracted from the listed boreholes in **Table S3**.

Table S3. List of boreholes used in the study to derive the relationship between soil organic depth and organic matter content (**Fig. S1**), covering the entire Mackenzie River Basin. The last column provides the number/name of the open file (OF) published by the Geological Survey of Canada, from which the data can be accessed.

ID	Name	Borehole	Borehole depth (m)	Lon.	Lat.	Peat depth (m)	Organic matter (%)	Source file
1	Inuvik Peatland	NTGS-BH01	11.25	-133.71	68.38	3.5	13.76	OF8652
2	Inuvik Hilltop	NTGS-BH02	20.5	-133.71	68.37	0.5	13.76	OF8652
3	Inuvik Riparian	NTGS-BH03	10.5	-133.70	68.37	3	13.76	OF8652
4	Jackfish Creek	JF-01	4.9	-128.47	66.29	0.8	29.70	OF6041
5	Jackfish Creek	JF-02	21.3	-128.47	66.28	0.2	29.70	OF6041
6	Fort Good Hope South	FGHS-01	10.2	-128.50	66.21	0.75	29.70	OF6041
7	Fort Good Hope South	FGHS-02	5.1	-128.50	66.21	0.2	29.70	OF6041
8	Snafu Creek	SC-01	19.8	-128.35	66.00	1.6	29.70	OF6041
9	Chick Lake	CL-01	21.3	-128.28	65.90	0.4	30.23	OF6041
10	Gibson Lake	GL-01	21.3	-127.89	65.75	0.6	35.59	OF6041
11	Hanna River	HR-01	21.3	-127.83	65.67	1.5	32.40	OF6041
12	Elliot Creek	EC-01	21.3	-127.62	65.52	2.3	32.89	OF6041
13	Elliot Creek	EC-03	12.2	-127.62	65.52	1.2	32.89	OF6041
14	Oscar Creek	OC-01	18.9	-127.44	65.44	0.6	35.37	OF6041
15	Billy Creek North	BCN-01	19.8	-127.32	65.40	0.25	33.86	OF6041
16	Vermillion Creek	VC-01	8.2	-126.14	65.10	0.6	33.29	OF6041
17	Vermillion Creek	VC-02	5.5	-126.13	65.10	1.5	33.29	OF6041
18	Police Island	PI-01	12.9	-125.01	64.83	0.25	25.98	OF6041
19	Old Fort Point	OFP-01	20	-124.84	64.65	0.2	26.92	OF6041
20	Little Smith Creek	LS-02	20	-124.73	64.43	0.2	27.04	OF6041
21	Saline River	SR-01	2.3	-123.68	63.47	0.25	29.22	OF6041
22	Saline River	SR-02	20.4	-124.49	64.29	0.2	25.17	OF6041
23	Steep Creek	Steep-03	20.7	-124.37	64.19	0.8	23.51	OF6041
24	Ochre River	OCR-01	1.5	-123.68	63.47	0.5	29.22	OF6041
25	Ochre River	OCR-02	2	-123.68	63.46	0.5	29.22	OF6041
26	River Between Two Mountains	RBTM-01	20.6	-123.20	62.95	0.2	23.11	OF6041
27	River Between Two Mountains	RBTM-02	12.5	-123.18	62.93	0.2	23.11	OF6041
28	Willowlake River	WLR-01	3.7	-123.08	62.71	0.2	69.46	OF6041
29	Ebbutt Hill	EH-01	16	-122.41	62.32	0.3	74.35	OF6041
30	Trail River	TR-01	12.2	-121.76	62.09	0.5	69.62	OF6041
31	Manners Sources	MS-01	16	-121.11	61.63	1.2	61.05	OF6041
32	Jean Marie Creek	JMC-01	8.5	-120.95	61.44	1.2	61.05	OF6041
33	Trout River	Trout R.	7.2	-120.59	61.02	0.5	50.60	OF6041
34	Trout Road Crossing	TRC	12	-120.48	60.83	0.5	51.35	OF6041

35	Pump Station 1	84-1-T4	14	-126.88	65.29	0.25	31.32	OF4635
36	Canyon Creek	84-2B-T4	20.5	-126.52	65.23	0.25	35.09	OF4635
37	Canyon Creek	84-2C-R4	20.5	-126.51	65.23	0.25	35.09	OF4635
38	Great Bear River	84-3A-G1	21	-125.58	64.91	0.25	32.10	OF4635
39	Great Bear River	84-3A-T4	9.1	-125.58	64.91	0.4	32.10	OF4635
40	Great Bear River	84-3B-G1	20.5	-125.58	64.91	0.25	32.10	OF4635
41	Great Bear River	84-3B-T4	20.25	-125.58	64.91	0.25	32.10	OF4635
42	Trail River	84-4A-T1	20	-121.99	62.07	1	64.69	OF4635
43	Trail River	84-4B-T4	20	-121.98	62.07	0.2	64.69	OF4635
44	Petitot River N.	84-5A-T3	20.5	-119.52	59.76	3.1	86.70	OF4635
45	Petitot River N.	84-5A-T4	20.5	-119.52	59.76	3.8	86.70	OF4635
46	Petitot River N.	84-5B-T3	20.5	-119.52	59.75	7	86.70	OF4635
47	Petitot River S.	84-6-G1	20.5	-119.25	59.46	2.9	86.70	OF4635
48	Petitot River S.	84-6-T3	20.5	-119.25	59.46	5.5	86.70	OF4635
49	Petitot River S.	84-6-T5	10	-119.25	59.46	5.2	86.70	OF4635
50	Table Mountain	85-7A-G1	20	-123.64	63.61	1.2	22.69	OF4635
51	Table Mountain	85-7A-T4	20	-123.64	63.61	0.5	22.69	OF4635
52	Table Mountain	85-7B-G1	20.25	-123.63	63.61	0.9	22.69	OF4635
53	Table Mountain	85-7C-T3	20.25	-123.63	63.60	0.3	22.69	OF4635
54	Manner's Creek	85-8A-G1	21	-121.09	61.60	0.4	61.05	OF4635
55	Manner's Creek	85-8A-T4	20	-121.09	61.60	0.5	61.05	OF4635
56	Manner's Creek	85-8B-G1	21	-121.09	61.60	2.7	61.05	OF4635
57	Manner's Creek	85-8B-T4	20	-121.09	61.60	2.4	61.05	OF4635
58	Manner's Creek	85-8C-G1	21	-121.09	61.60	1.6	61.05	OF4635
59	Manner's Creek	85-8C-T4	21	-121.09	61.60	1.3	61.05	OF4635
60	Mackenzie Hwy. S.	85-10A-G1	5.8	-120.87	61.35	0.8	61.05	OF4635
61	Mackenzie Hwy. S.	85-10B-G1	5.2	-120.86	61.35	3	61.05	OF4635
62	Mackenzie Hwy. S.	85-10B-T3	10.75	-120.86	61.35	2.7	61.05	OF4635
63	Mackenzie Hwy. S.	85-10B-T4	10.75	-120.86	61.35	2.3	61.05	OF4635
64	Moraine South	85-11-G1	14.25	-120.80	61.28	0.5	61.05	OF4635
65	Moraine South	85-11-T4	12.75	-120.80	61.28	0.5	61.05	OF4635
66	Jean Marie Creek	85-12A-G1	12.25	-120.42	61.11	0.5	58.91	OF4635
67	Jean Marie Creek	85-12A-T4	12.25	-120.42	61.11	1.2	58.91	OF4635
68	Jean Marie Creek	85-12B-G1	16.8	-120.42	61.11	2.9	58.91	OF4635
69	Jean Marie Creek	85-12B-T3	16.8	-120.42	61.11	3.2	58.91	OF4635
70	Jean Marie Creek	85-12B-T4	10.8	-120.42	61.11	4.8	58.91	OF4635
71	Redknife Hills	85-13A-T1	20.5	-120.29	60.57	1.6	76.25	OF4635
72	Redknife Hills	85-13B-T1A	10.5	-120.29	60.56	1.25	76.25	OF4635
73	Redknife Hills	85-13C-T1	6.4	-120.29	60.56	4.9	76.25	OF4635

S2. Climate forcing processing

Given that the utilized temporal disaggregation routine does not preserve the diurnal cycle of specific humidity, it was a must to modify the processed values to overcome any possible oversaturation (*i.e.* relative humidity exceeding 100%) and negative evapotranspiration (condensation) events, as shown in **Fig. S2**.

According to (Gill, 1982), specific humidity in the air is given as:

$$q_a = \frac{0.622 \times e_a}{P_a - 0.378 \times e_a} \qquad \text{Equ. (1)}$$

where q_a is the specific humidity (kg/kg), P_a is surface pressure (Pa), and e_a is the vapour pressure (Pa) of the air, calculated as:

$$e_a = RH \times 10^{\left[\frac{(0.7859 + 0.03477 \times T_a)}{(1.0 + 0.00412 \times T_a)} + 2\right]} \qquad \text{Equ. (2)}$$

where T_a is the air temperature (°C) and RH is the relative humidity (%). Manipulating equations (1) and (2) leads to the following equation that relates specific humidity, relative humidity, air temperature and surface pressure:

$$RH = \frac{(q_a \times P_a)/(0.378 q_a + 0.622)}{10^{[2 + (0.7859 + 0.03477 T_a)/(1 + 0.00412 T_a)]}} \qquad \text{Equ. (3)}$$
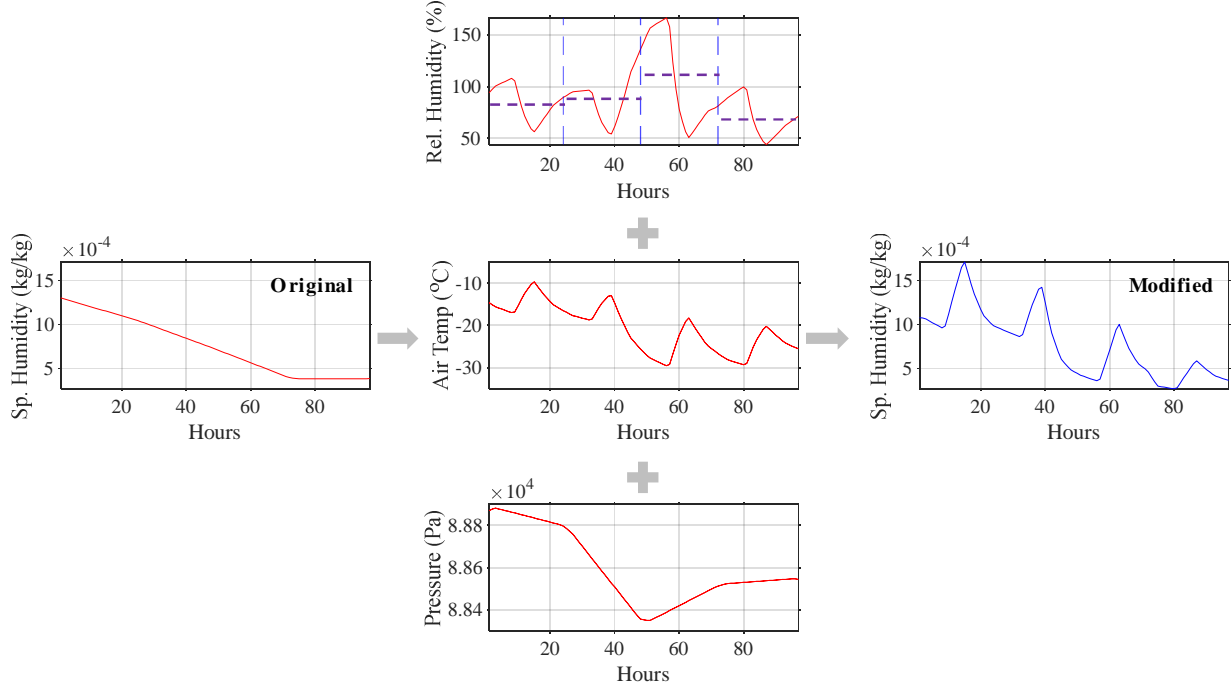
Fig. S2. Specific humidity processing to impose the diurnal cycle.

S3. Preliminary hydrologic assessment

Four gauge stations are incorporated in the current study to assess the quality of streamflow simulation (**Table S4**). As a preliminary check, streamflow simulation is evaluated under the original LRB parameterization (based on GEM-CaPA) under W5E5 V2 forcing dataset at the four stations (**Fig. 5** in the main manuscript, **Fig. S3**, **Fig. S4**, and **Fig. S5**). Further, the partitioning of surface water-balance and subsurface water-balance components under the two forcing datasets is provided in **Fig. S6** and **Fig. S7**.

Table S4. Streamflow gauge stations used in the current study.

Station ID	Station Name	Area (km^2)	Data availability	Note
10AA001	Liard at Upper Crossing	32,556	1960-2019	Headwater
10BE001	Liard at Lower Crossing	104,355	1944-2019	Intermediate
10ED001	Liard at Fort Liard	218,808	1942-2021	Intermediate
10ED002	Liard near the mouth	274,164	1972-2021	Outlet
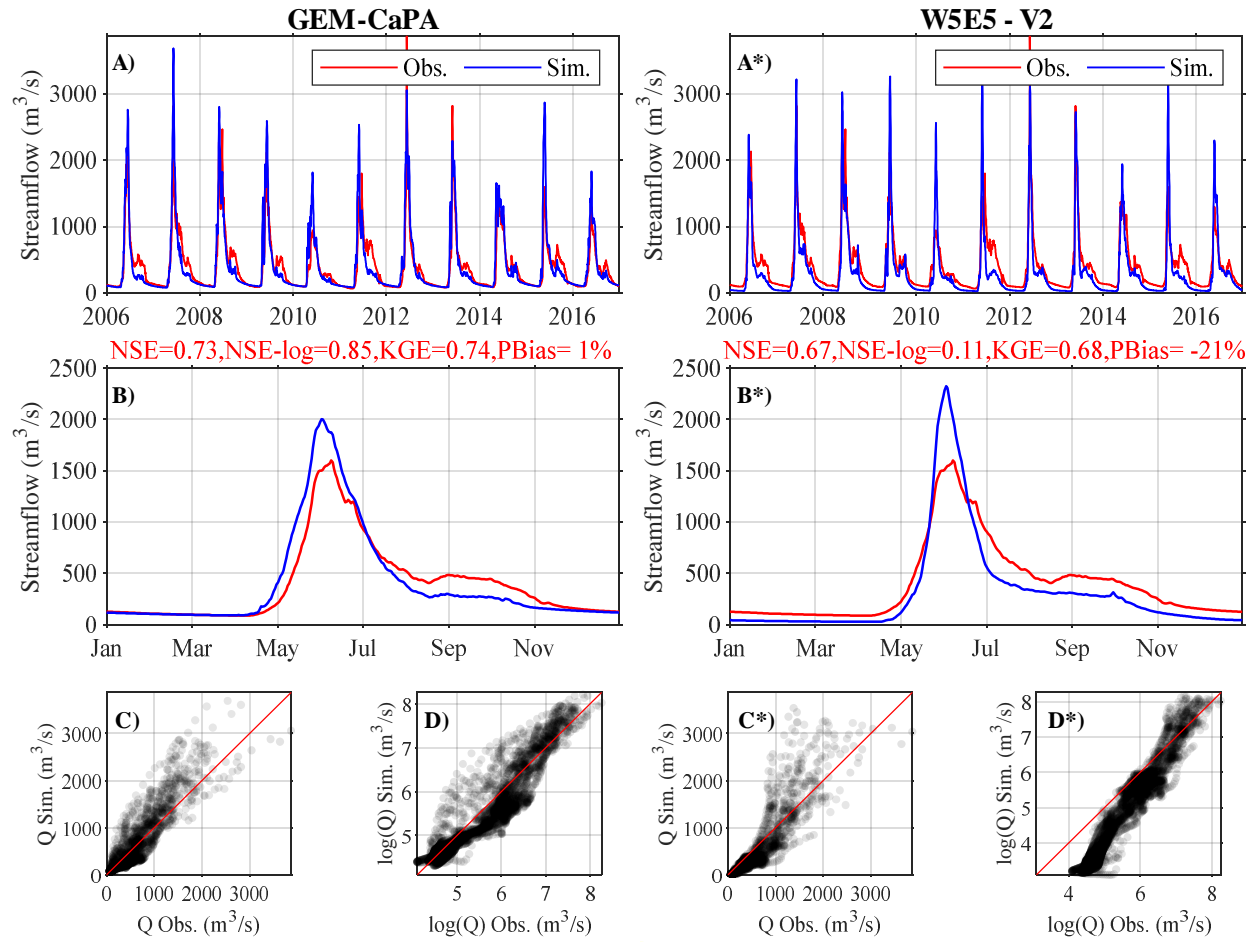
Fig. S3. Same as **Fig. 5**, but showing station 10AA001 (LRB Headwater).
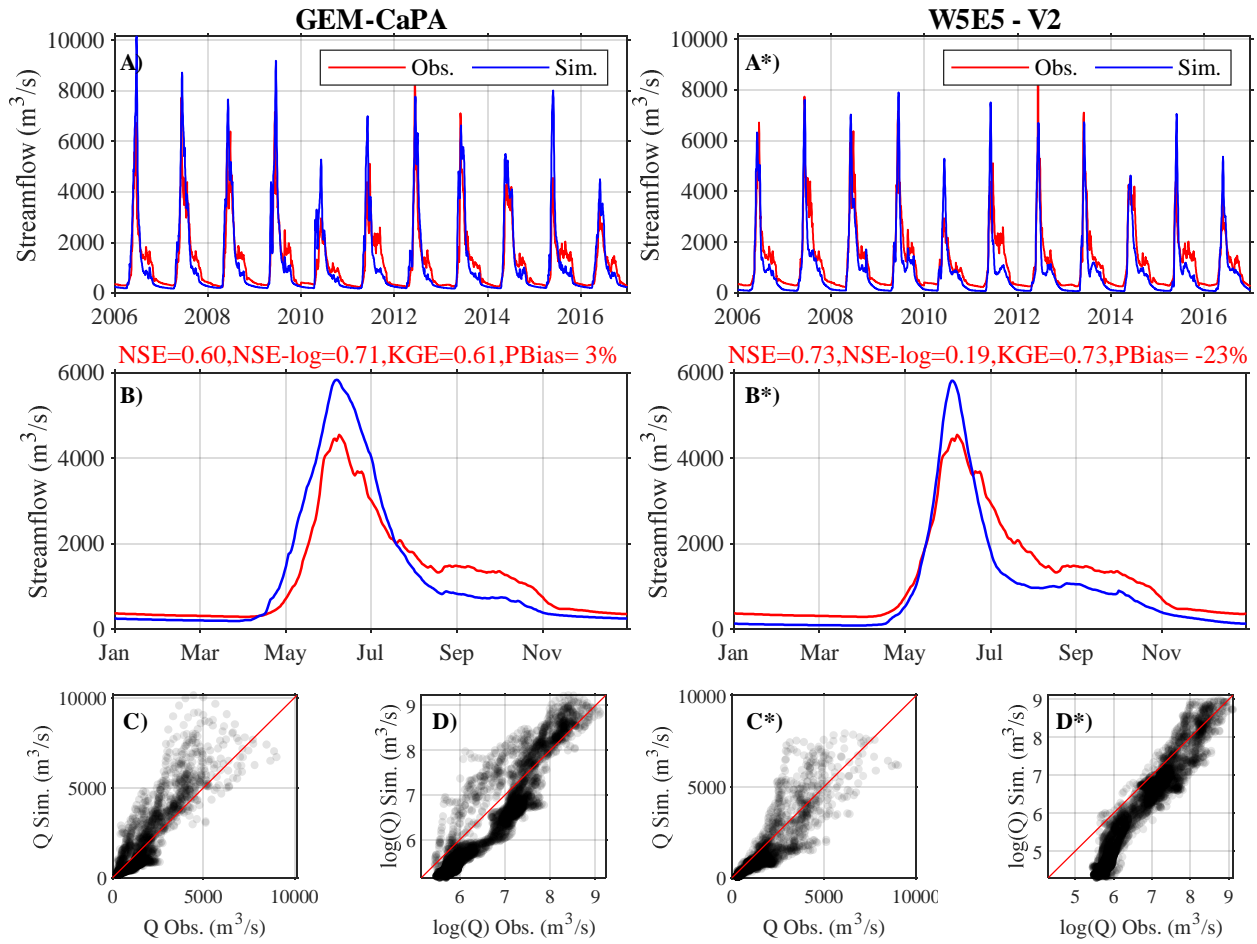
Fig. S4. Same as **Fig. 5**, but showing station 10BE001 (LRB Intermediate).
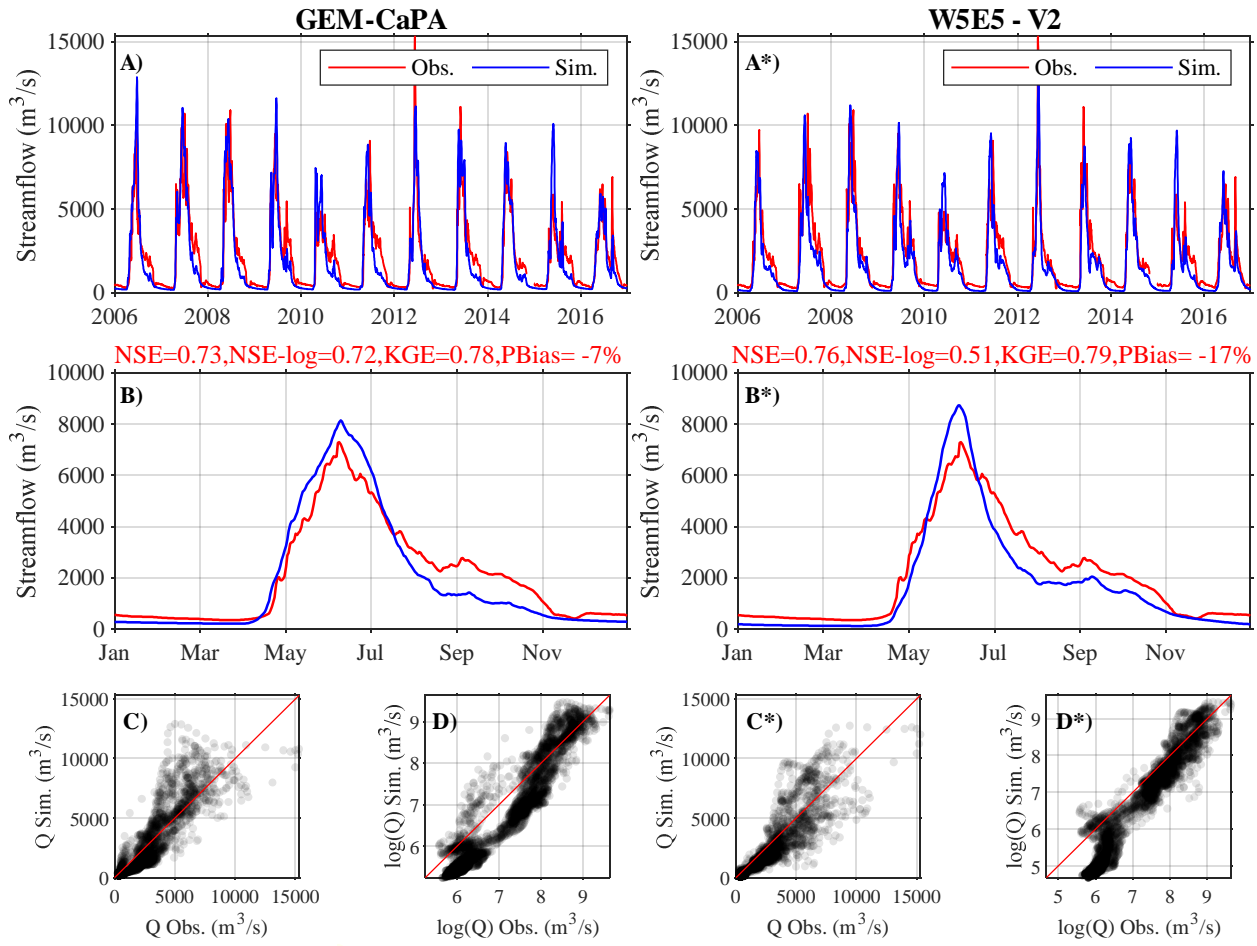
Fig. S5. Same as **Fig. 5**, but showing station 10ED001 (LRB Intermediate).
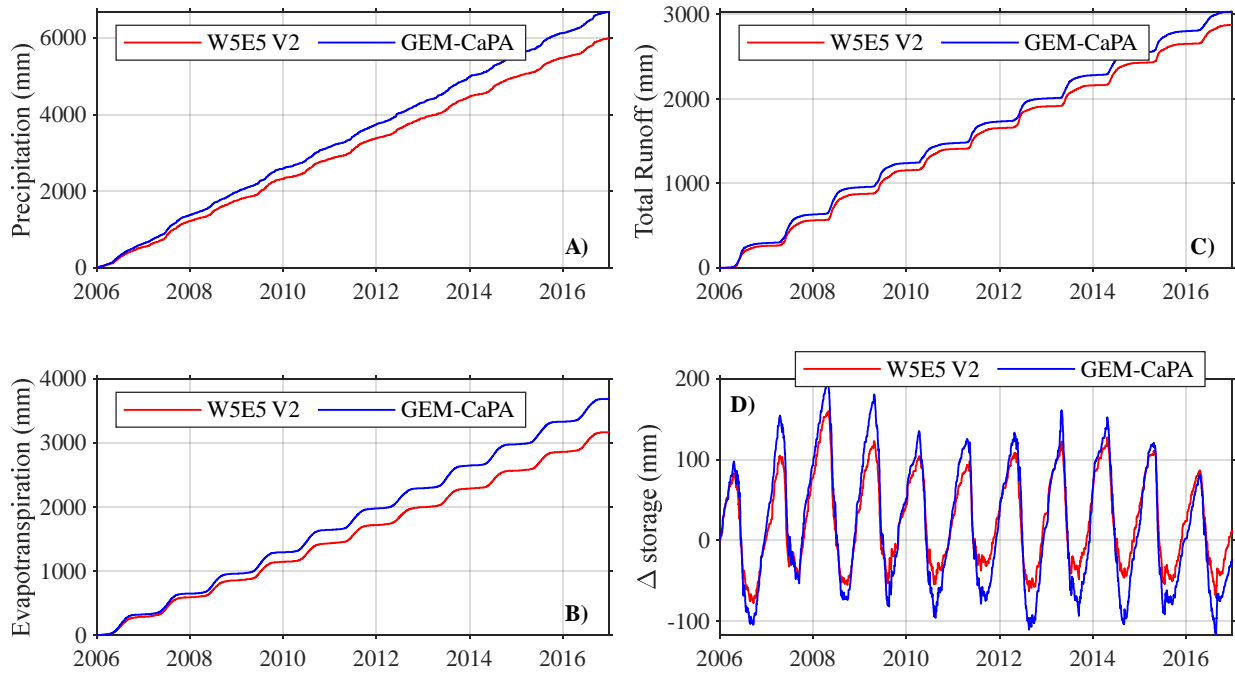
Fig. S6. The partitioning of water-balance components for the same model configuration under W5E5 V2 and GEM-CaPA forcings into A) cumulative precipitation, B) cumulative evapotranspiration, C) total runoff, and D) the change in total storage (including soil, canopy, ponding, and snow). The provided water equivalent depths (mm) correspond to the basin average with a daily time-step.
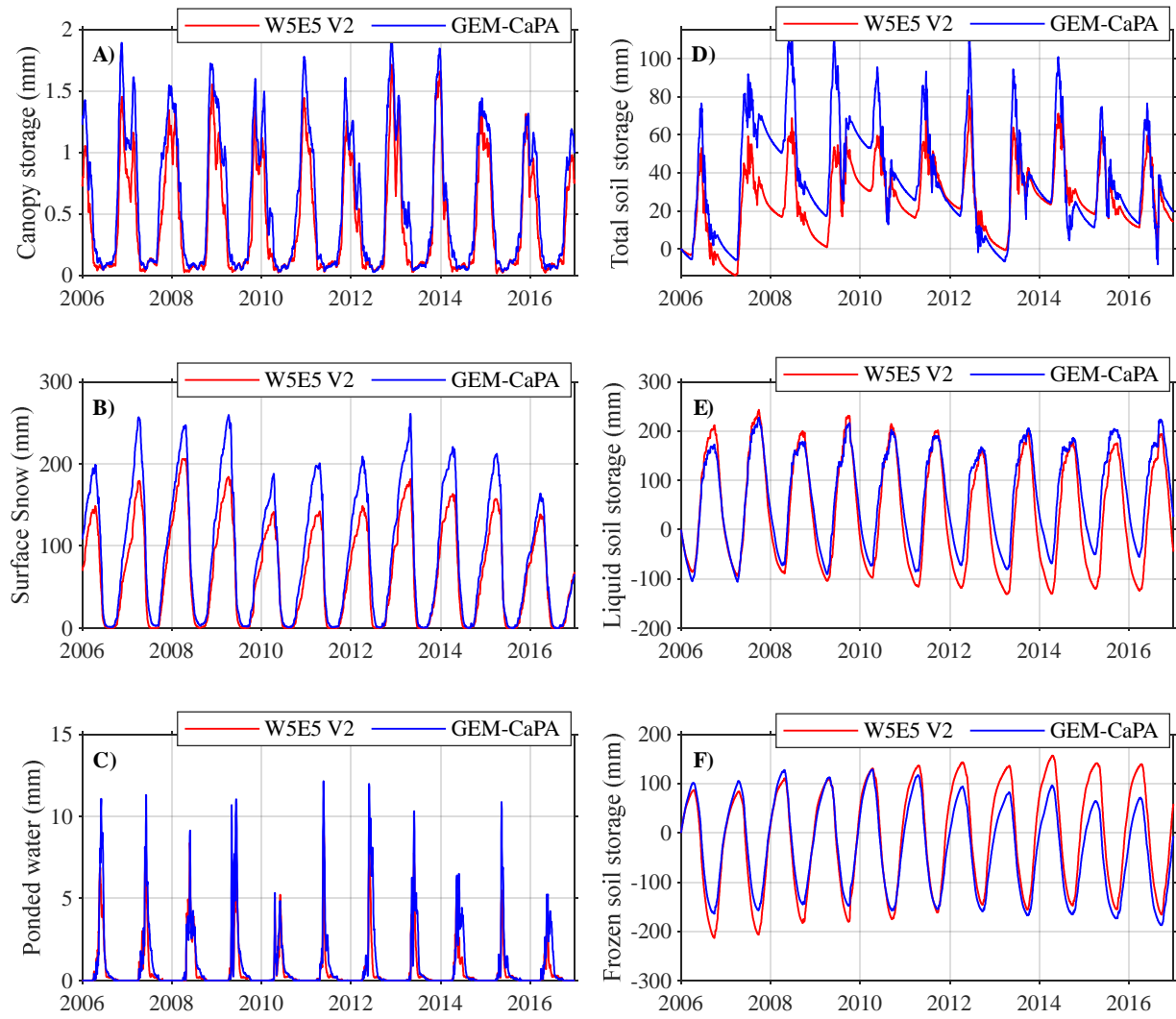
Fig. S7. The partitioning of basin-storage for the same model configuration under W5E5 V2 and GEM-CaPA forcings into A) canopy storage, B) surface snow, C) ponded water, D) total soil storage, E) liquid soil water storage, and F) frozen soil water storage. The provided water equivalent depths (mm) correspond to the basin average with a daily time-step.

S4. Ground observations assessment

Figs. S8-16 show the observed and simulated temperature envelopes (and the associated variability range) for the employed permafrost sites for a selected year (varies across sites depending on available records), while the performance metrics for T_{min} and T_{max} envelopes for all experiments are presented in **Tables S5-13**. Similarly, **Table S14** summarizes the quality of simulated ALT for the Manners Creek sites.
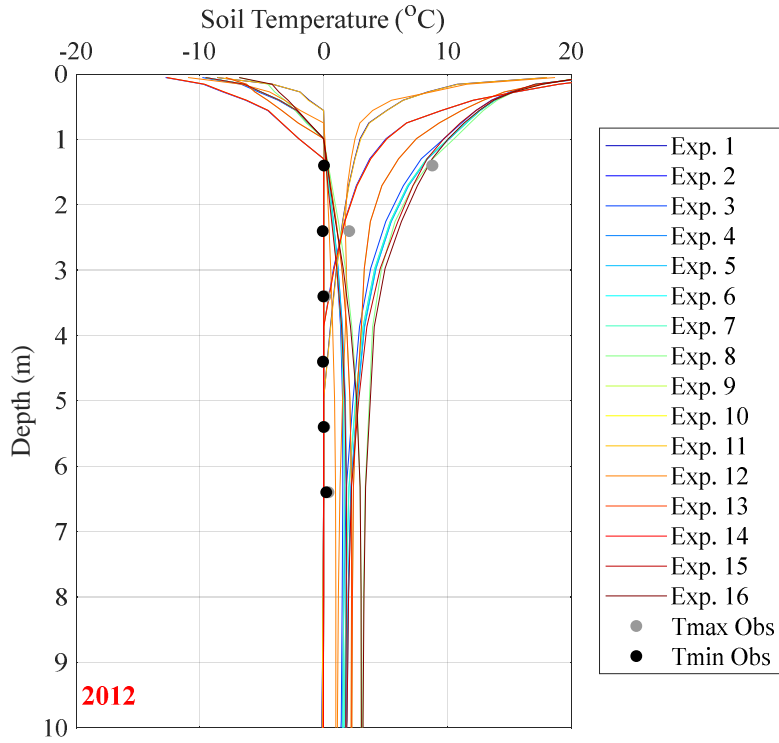
Fig. S8. Same as **Fig. 6**, but showing Scotty Creek (Fen) for Wetland GRU in 2012.

Table S5. Same as **Table 4**, but reporting Scotty Creek (Fen) site for Wetland GRU.

Exp. Id	Tmin			Tmax		
	RMSE	BIAS	MAE	RMSE	BIAS	MAE
1	0.27	0.17	0.20	4.77	2.73	2.74
2	0.40	0.26	0.29	4.14	2.48	2.51
3	1.00	-0.92	0.92	3.07	-0.28	2.35
4	1.17	-1.06	1.07	3.09	-0.65	2.50
5	1.19	-1.08	1.08	3.10	-0.67	2.52
6	1.07	-0.98	0.98	3.05	-0.54	2.43
7	1.07	-0.98	0.98	3.05	-0.54	2.43
8	2.08	-1.92	1.92	3.42	-1.70	3.08
9	1.60	-1.49	1.49	3.31	-0.36	2.63
10	0.39	0.26	0.28	4.11	2.45	2.50
11	0.27	0.17	0.20	4.75	2.69	2.74
12	0.56	-0.52	0.52	4.22	1.34	2.62
13	1.60	-1.49	1.49	3.31	-0.36	2.63
14	0.39	0.26	0.28	4.11	2.45	2.50
15	1.14	-1.03	1.03	3.19	-0.81	2.59
16	2.02	-1.84	1.84	3.54	-1.84	3.23
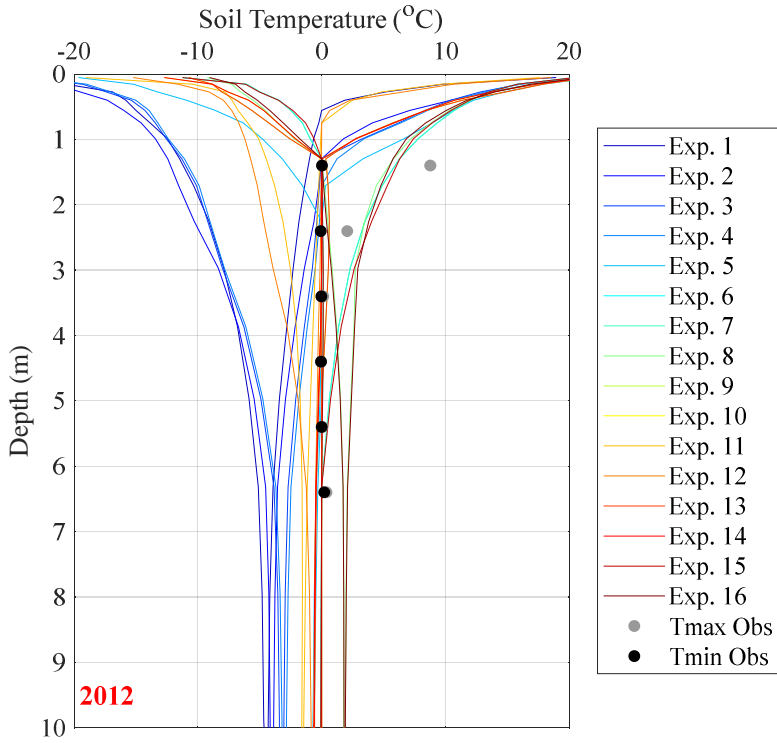
Fig. S9. Same as **Fig. 6**, but showing Scotty Creek (Fen) for Needleleaf Forest GRU in 2012.

Table S6. Same as **Table 4**, but reporting Scotty Creek (Fen) site for Needleleaf Forest GRU.

Exp. Id	Tmin			Tmax		
	RMSE	BIAS	MAE	RMSE	BIAS	MAE
1	8.18	7.81	7.81	7.16	6.08	6.08
2	8.21	7.65	7.65	6.52	5.41	5.41
3	7.34	6.84	6.84	6.21	4.81	4.81
4	7.15	6.64	6.64	5.74	4.45	4.45
5	1.20	0.76	0.76	4.51	2.93	2.93
6	0.26	0.14	0.19	3.18	1.44	1.87
7	0.26	0.14	0.19	3.18	1.44	1.87
8	1.10	-0.99	0.99	3.19	-0.20	2.45
9	0.27	0.18	0.20	4.65	2.71	2.73
10	0.65	0.49	0.49	5.36	3.38	3.38
11	2.43	2.28	2.28	5.98	4.11	4.11
12	1.81	1.67	1.67	5.82	3.63	3.63
13	0.27	0.18	0.20	4.65	2.71	2.73
14	0.65	0.49	0.49	5.36	3.38	3.38
15	0.29	0.10	0.23	3.22	1.17	1.94
16	1.07	-0.94	0.95	3.26	-0.31	2.52
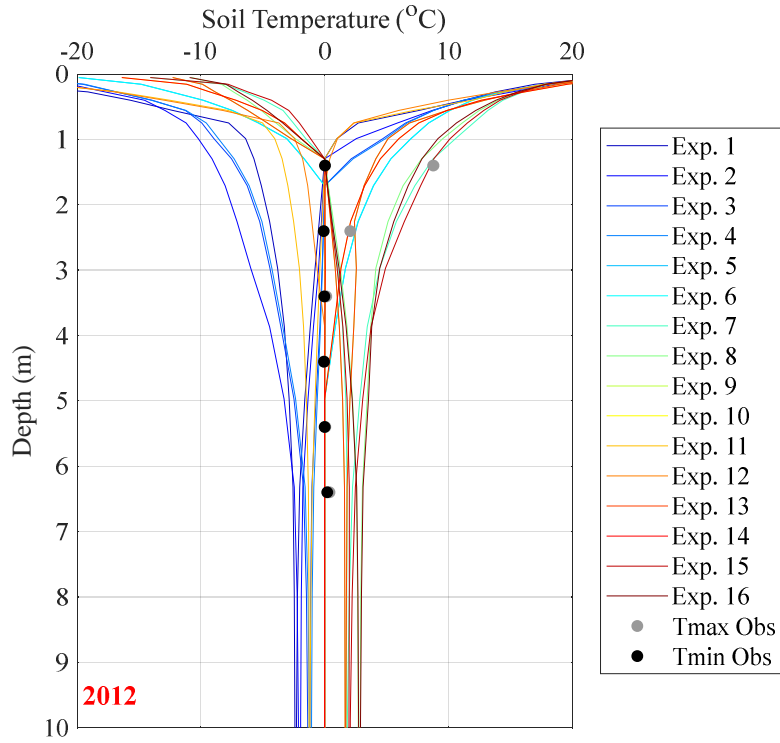
Fig. S10. Same as **Fig. 6**, but showing Scotty Creek (Fen) for Broadleaf Forest GRU in 2012.

Table S7. Same as **Table 4**, but reporting Scotty Creek (Fen) site for Broadleaf Forest GRU.

Exp. Id	Tmin			Tmax		
	RMSE	**BIAS**	**MAE**	**RMSE**	**BIAS**	**MAE**
1	4.47	4.27	4.27	6.09	4.54	4.54
2	5.78	5.24	5.24	6.01	4.34	4.34
3	4.74	4.24	4.24	5.10	3.54	3.54
4	4.56	4.07	4.07	5.02	3.44	3.44
5	0.74	0.45	0.47	3.61	1.98	2.22
6	0.73	0.45	0.47	3.61	1.98	2.22
7	1.16	-1.02	1.05	3.07	-0.85	2.54
8	1.72	-1.54	1.54	3.40	-1.49	2.97
9	1.05	-0.94	0.94	3.44	0.29	2.51
10	0.37	0.25	0.27	3.84	2.16	2.32
11	2.55	2.42	2.42	5.88	3.96	3.96
12	0.61	0.45	0.46	5.56	3.30	3.30
13	1.05	-0.94	0.94	3.44	0.29	2.51
14	0.37	0.25	0.27	3.84	2.16	2.32
15	1.24	-1.09	1.09	3.24	-1.13	2.74
16	1.68	-1.48	1.49	3.52	-1.65	3.14
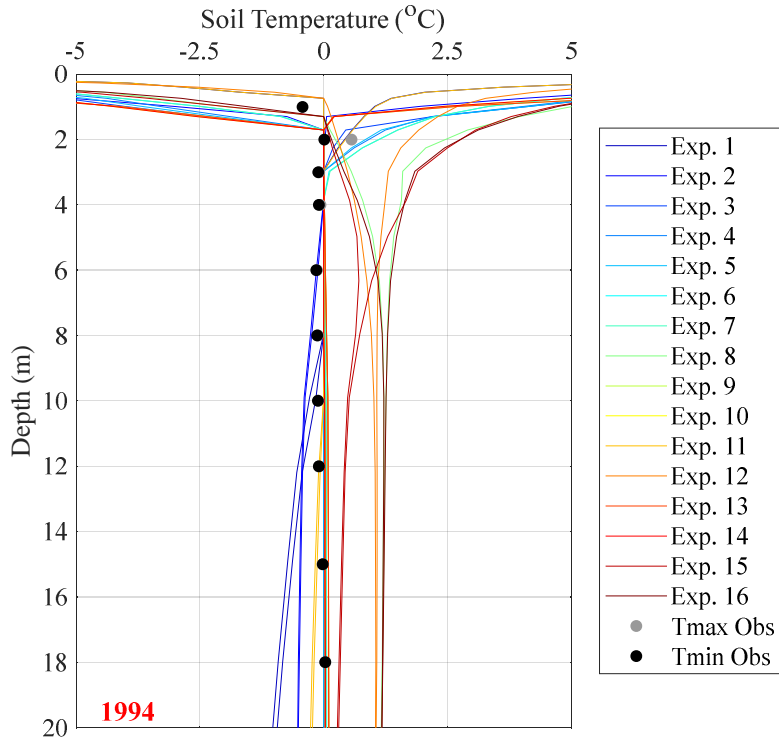
Fig. S11. Same as **Fig. 6**, but showing Petitot River North (84-5A-T4) for Wetland GRU in 1994.

Table S8. Same as **Table 4**, but reporting Petitot River North (84-5A-T4) for Wetland GRU.

Exp. Id	Tmin			Tmax		
	RMSE	BIAS	MAE	RMSE	BIAS	MAE
1	1.08	0.81	0.87	1.31	0.78	0.86
2	0.63	0.43	0.47	0.87	0.45	0.54
3	0.54	0.05	0.26	0.78	-0.13	0.34
4	0.55	0.05	0.27	0.85	-0.19	0.37
5	0.55	0.05	0.27	0.84	-0.19	0.36
6	0.58	0.03	0.29	0.93	-0.29	0.46
7	0.58	0.03	0.29	0.93	-0.29	0.46
8	1.11	-0.98	1.06	1.94	-1.66	1.71
9	0.29	-0.11	0.20	0.69	0.08	0.33
10	0.52	0.08	0.29	0.75	0.10	0.33
11	0.42	0.24	0.33	1.00	0.38	0.50
12	0.97	-0.93	0.93	1.53	-1.09	1.39
13	0.29	-0.11	0.20	0.69	0.08	0.33
14	0.52	0.08	0.29	0.75	0.10	0.33
15	0.57	-0.13	0.37	1.25	-0.77	0.86
16	1.08	-0.96	1.01	2.01	-1.71	1.77
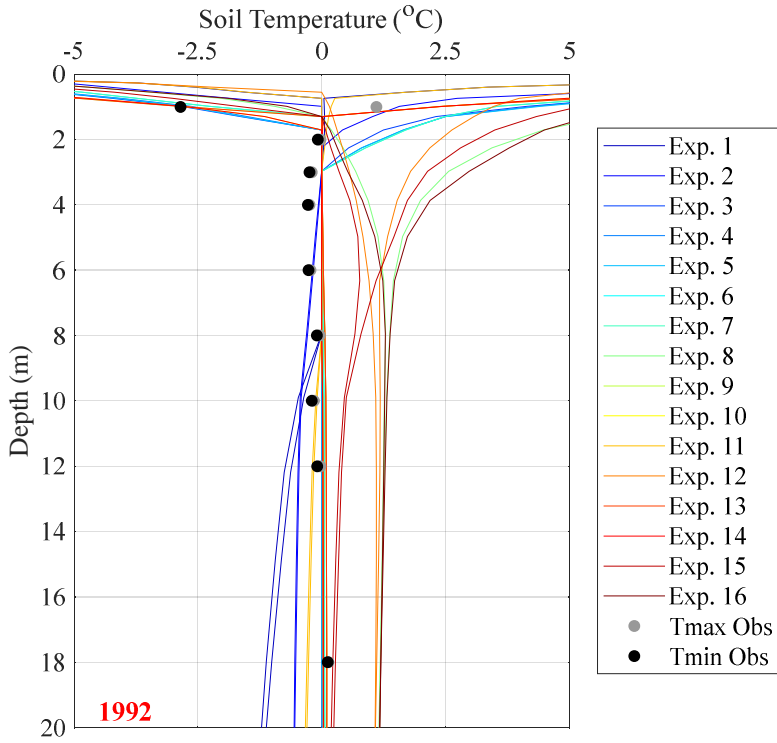
Fig. S12. Same as **Fig. 6**, but showing Petitot River North (84-5B-T4) for Wetland GRU in 1992.

Table S9. Same as **Table 4**, but reporting Petitot River North (84-5B-T4) for Wetland GRU.

Exp. Id	Tmin			Tmax		
	RMSE	BIAS	MAE	RMSE	BIAS	MAE
1	1.32	0.43	1.21	0.98	0.52	1.05
2	0.98	0.13	0.72	0.70	0.12	0.57
3	0.76	-0.20	0.42	1.30	-0.52	0.55
4	0.69	-0.20	0.40	1.39	-0.57	0.58
5	0.69	-0.20	0.39	1.41	-0.57	0.58
6	0.73	-0.22	0.42	1.36	-0.58	0.58
7	0.74	-0.22	0.42	1.36	-0.58	0.58
8	1.38	-1.22	0.97	2.64	-2.15	1.90
9	0.60	-0.34	0.30	0.56	-0.27	0.31
10	0.79	-0.18	0.40	0.62	-0.25	0.33
11	0.85	-0.05	0.50	0.53	0.09	0.47
12	1.38	-1.16	0.90	1.72	-1.53	1.35
13	0.60	-0.34	0.30	0.56	-0.27	0.31
14	0.79	-0.18	0.40	0.62	-0.25	0.33
15	0.82	-0.42	0.35	1.79	-1.12	0.48
16	1.37	-1.19	0.94	2.67	-2.21	1.94
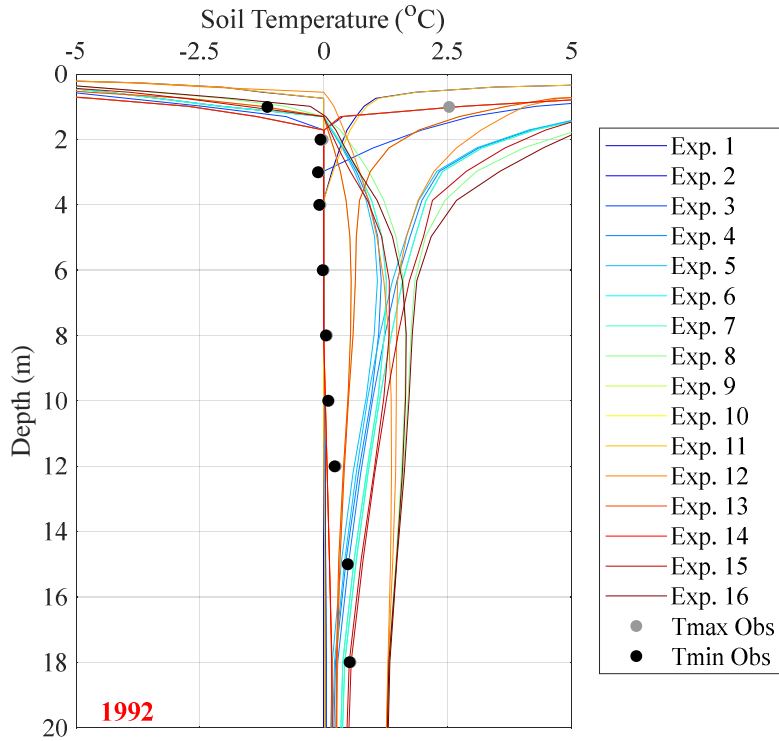
Fig. S13. Same as **Fig. 6**, but showing Petitot River South (84-6-T6) for Wetland GRU in 1992.

Table S10. Same as **Table 4**, but reporting Petitot River South (84-6-T6) for Wetland GRU.

Exp. Id	Tmin			Tmax		
	RMSE	**BIAS**	**MAE**	**RMSE**	**BIAS**	**MAE**
1	0.26	0.18	0.30	0.58	0.05	0.41
2	0.33	0.26	0.34	0.66	0.05	0.44
3	0.32	0.23	0.31	1.16	-0.21	0.74
4	0.46	-0.10	0.54	2.04	-1.15	1.49
5	0.44	-0.02	0.50	1.95	-1.03	1.36
6	0.48	-0.25	0.59	2.18	-1.37	1.69
7	0.48	-0.25	0.59	2.18	-1.37	1.69
8	0.70	-1.01	1.04	2.54	-2.03	2.30
9	0.23	-0.08	0.31	0.79	-0.35	0.71
10	0.31	0.24	0.29	0.61	0.01	0.39
11	0.24	0.14	0.26	0.57	0.03	0.40
12	0.61	-0.93	0.93	1.72	-1.50	1.64
13	0.23	-0.08	0.31	0.79	-0.35	0.71
14	0.31	0.24	0.29	0.61	0.01	0.39
15	0.47	-0.37	0.59	2.32	-1.57	1.83
16	0.68	-0.99	0.99	2.62	-2.12	2.37
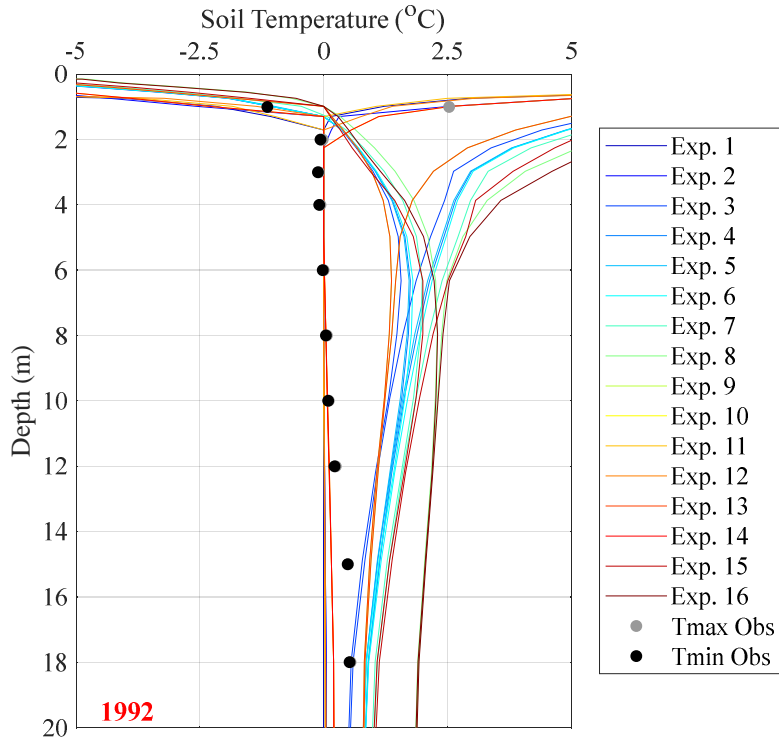
Fig. S14. Same as **Fig. 6**, but showing Petitot River South (84-6-T6) for Shrubs GRU in 1992.

Table S11. Same as **Table 4**, but reporting Petitot River South (84-6-T6) for Shrubs GRU.

Exp. Id	Tmin			Tmax		
	RMSE	**BIAS**	**MAE**	**RMSE**	**BIAS**	**MAE**
1	0.53	0.64	0.68	0.49	0.25	0.42
2	0.26	0.19	0.28	0.55	0.08	0.37
3	0.55	-0.61	0.73	2.48	-1.68	1.97
4	0.63	-0.82	0.85	2.74	-2.00	2.22
5	0.63	-0.81	0.84	2.74	-2.00	2.20
6	0.64	-0.83	0.87	2.76	-2.02	2.23
7	0.71	-0.98	0.99	2.93	-2.22	2.39
8	1.04	-1.57	1.57	3.25	-2.75	2.98
9	0.55	-0.76	0.76	1.82	-1.37	1.57
10	0.24	0.13	0.23	0.57	-0.02	0.36
11	0.41	0.39	0.46	0.45	0.18	0.33
12	0.32	0.28	0.34	0.44	0.16	0.31
13	0.55	-0.76	0.76	1.82	-1.37	1.57
14	0.24	0.13	0.23	0.57	-0.02	0.36
15	0.70	-0.97	0.97	3.03	-2.34	2.49
16	1.00	-1.51	1.51	3.32	-2.83	3.04
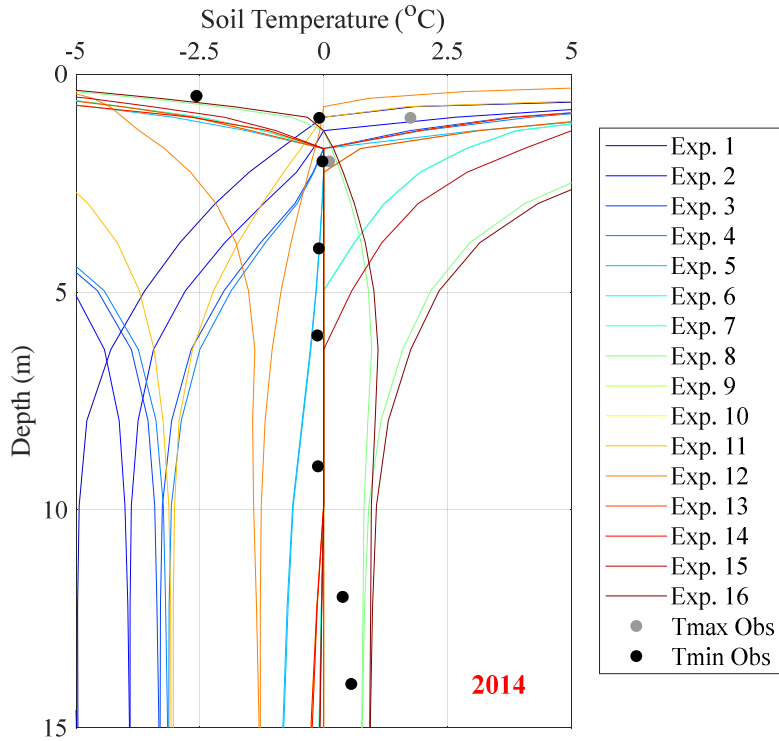
Fig. S15. Same as **Fig. 6**, but showing Wrigley Highway (99TC03) for Needleleaf Forest GRU in 2014.

Table S12. Same as **Table 4**, but reporting Wrigley Highway (99TC03) for Needleleaf Forest GRU.

Exp. Id	Tmin			Tmax		
	RMSE	**BIAS**	**MAE**	**RMSE**	**BIAS**	**MAE**
1	13.04	12.14	12.14	5.51	0.64	5.20
2	11.46	10.46	10.46	4.95	-0.65	4.60
3	10.69	9.68	9.68	4.65	-1.25	4.38
4	10.47	9.48	9.48	4.59	-1.39	4.34
5	3.55	2.70	2.71	4.00	-2.66	3.48
6	2.92	2.25	2.33	4.49	-3.51	3.81
7	2.92	2.25	2.33	4.49	-3.51	3.81
8	2.65	1.62	2.42	5.45	-4.75	4.75
9	3.45	2.59	2.67	4.13	-3.24	3.51
10	4.07	3.11	3.18	4.07	-2.99	3.45
11	7.78	7.17	7.17	4.32	-0.52	4.13
12	4.95	4.59	4.59	4.11	-0.70	3.61
13	3.45	2.59	2.67	4.13	-3.24	3.51
14	4.07	3.11	3.18	4.07	-2.99	3.45
15	2.58	2.00	2.09	4.48	-3.59	3.88
16	2.59	1.48	2.42	5.44	-4.82	4.82
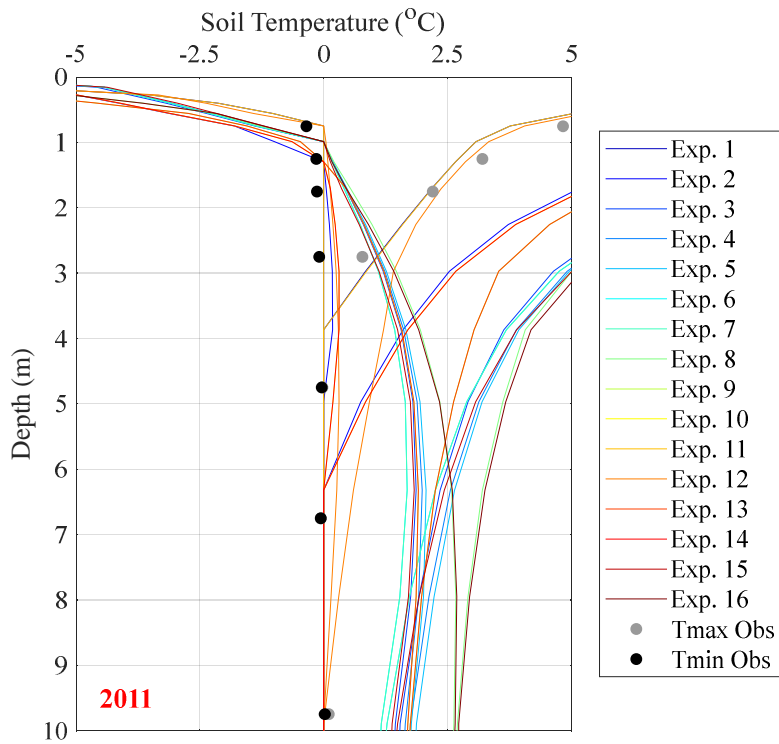
Fig. S16. Same as **Fig. 6**, but showing Liard Spruce (97TC04) site for Wetland GRU in 1992.

Table S13. Same as **Table 4**, but reporting Liard Spruce (97TC04) for Wetland GRU.

Exp. Id	Tmin			Tmax		
	RMSE	BIAS	MAE	RMSE	BIAS	MAE
1	3.23	0.86	2.26	3.81	-1.38	2.94
2	2.82	1.38	2.14	4.80	-4.05	4.14
3	2.94	0.11	2.46	6.41	-5.87	5.96
4	2.97	0.00	2.48	6.62	-6.09	6.17
5	2.99	-0.03	2.52	6.65	-6.14	6.22
6	2.87	0.15	2.35	6.47	-5.88	5.97
7	2.87	0.15	2.35	6.47	-5.88	5.97
8	3.18	-0.31	2.76	7.15	-6.68	6.77
9	2.99	0.38	2.67	5.98	-5.54	5.63
10	2.81	1.34	2.15	4.85	-4.11	4.20
11	3.24	0.86	2.26	3.81	-1.40	2.94
12	3.37	0.95	2.52	3.84	-2.06	3.24
13	2.99	0.38	2.67	5.98	-5.54	5.63
14	2.81	1.34	2.15	4.85	-4.11	4.20
15	2.90	0.06	2.39	6.57	-6.01	6.11
16	3.19	-0.34	2.73	7.20	-6.73	6.83

Table S14. Same as **Table 4**, but reporting the performance metrics for the ALT of Manners Creek (92TT-5 and 92TT-4) for Needleleaf Forest GRU.

Exp. Id	92TT-5			92TT-4		
	RMSE	BIAS	MAE	RMSE	BIAS	MAE
1	2.99	-0.77	0.77	1.02	-0.26	0.26
2	1.81	-0.47	0.47	0.31	0.08	0.09
3	1.81	-0.47	0.47	0.31	0.08	0.09
4	1.39	-0.36	0.37	0.84	0.22	0.22
5	0.44	-0.11	0.14	1.90	0.49	0.49
6	1.27	0.33	0.33	3.89	1.00	1.00
7	1.27	0.33	0.33	3.89	1.00	1.00
8	16.76	4.33	4.37	23.33	6.02	6.02
9	1.60	-0.41	0.41	0.73	0.19	0.19
10	1.81	-0.47	0.47	0.31	0.08	0.09
11	2.92	-0.75	0.75	0.96	-0.25	0.25
12	4.00	-1.03	1.03	2.17	-0.56	0.56
13	1.60	-0.41	0.41	0.73	0.19	0.19
14	1.81	-0.47	0.47	0.31	0.08	0.09
15	2.00	0.52	0.52	4.99	1.29	1.29
16	4.83	1.25	1.29	5.81	1.50	1.50

S5. Gridded products assessment

S5.1. Permafrost zonation

Fig. S17 compares the spatial pattern of permafrost zonation for all gridded datasets. Most datasets agree to some extent that continuous (extent ≥ 0.9) and discontinuous ($0.9 \geq$ extent ≥ 0.5) zones are found in the northern half of the basin, except the Obu et al. (2019) dataset that mapped these zones in the northern, eastern, and southern parts of the basin, and Ran et al. (2022) that mapped these zones in the northern and southern parts of the basin. However, all datasets disagree on the partitioning of continuous and discontinuous zones, which was also shown in **Fig.4**. However, all datasets differed in the spatial extent and distribution of the sporadic ($0.5 \geq$ extent ≥ 0.1) and isolated patches zones (extent < 0.1) zones, which was also highlighted in **Fig.4**.
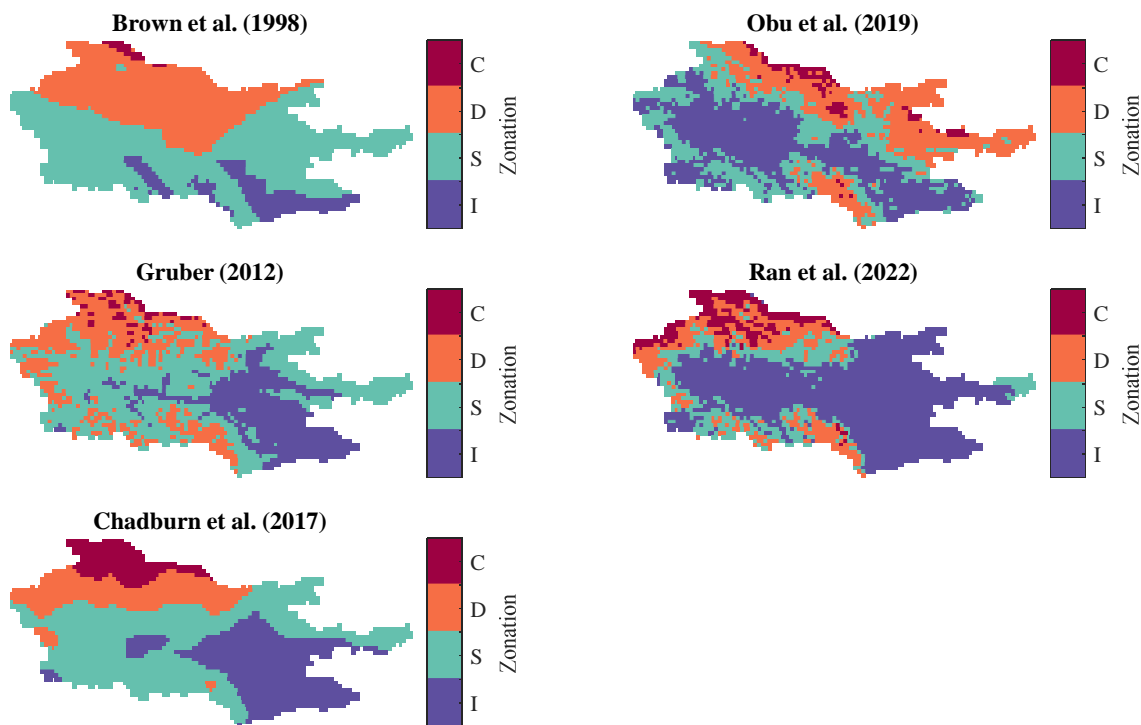
Fig. S17. Permafrost zonation based on different gridded products for the LRB; "C" denotes Continuous permafrost; "D" denotes Discontinuous Permafrost; "S" denotes Sporadic Permafrost; "I" denotes Isolated Patches of Permafrost.

S5.2. Permafrost Area

The permafrost area (PA) is another important indicator and valuable by-product that has been incorporated in most permafrost-related studies (*e.g.* Burke et al., 2020; Ji et al., 2022; Melton et al., 2019). **Fig. S18** presents the time series of the simulated PA for all the experiments, in conjunction with the gridded datasets PA, where each dataset is plotted as a straight line (corresponding to its representative period – see **Table 2** in the main document) or an envelope of the area over the representative period (for Brown et al. (1998) and Chadburn et al. (2017)). It is worth noting that Brown et al. (1998) dataset was excluded from the extent assessment as it only provides the boundary of each permafrost zonation without any information about the permafrost extent (PE) variability (or probability) within each zone; still, it could be beneficial in assessing the total area, given that this dataset had always been a cornerstone in developing and evaluating most of the available permafrost gridded products. Several experiments can be eliminated based on their overestimated PA, as shown in **Fig. 8** in the main document. These experiments are Exp.1-5 and 11, which have a total area $> 162,000$ km^2 (*i.e.,* the upper bound of Brown et al. (1998)). Besides, the total area based on Ran et al. (2022) has not been fulfilled by any of the experiments. Noting that this product has the smallest permafrost area among all the datasets (~62,000 km^2) with a relatively odd distribution of permafrost zones/extent (see **Fig. 4** in the main document).

The remaining experiments (after excluding 1, 5, and 11) can be classified into three groups: (1) satisfying one dataset: Exp.10,14, 6, and 12 that lie within the band of variability of Brown et al. (1998), but exceed the upper bound of Chadburn et al. (2017), (2) satisfying two datasets: Exp.7, 15, 9, 13, 8, and 16 with respect to Brown et al. (1998), and Chadburn et al. (2017) datasets, and (3) satisfying three datasets: Exp.8 and 16 with respect to Brown et al. (1998), Obu et al. (2019), and Chadburn et al. (2017) datasets. Exp.16 is also the closest one to Gruber (2012) dataset.
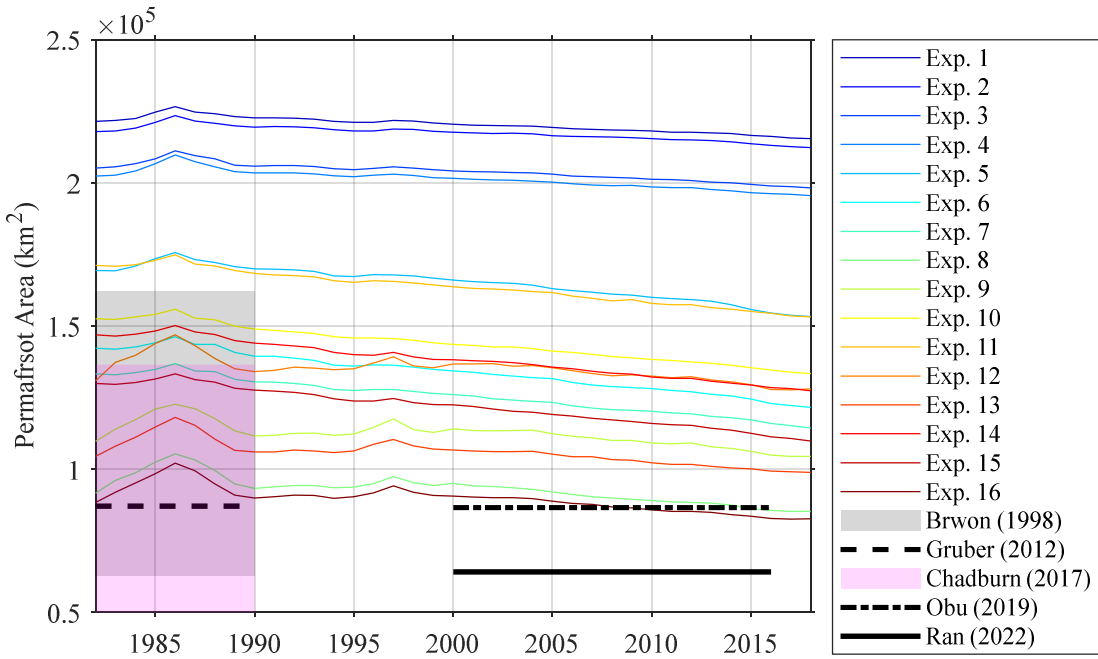
Fig. S18. Temporal evolution of the simulated permafrost area, in addition to the gridded-based permafrost area; the range of variability for Brown and Chadburn datasets is highlighted using a shaded area. Refer to **Table 3** (in the main document) for further information about the configured experiments.

The Cumulative frequency distribution (CDF) of the simulated and the gridded datasets PE is provided in **Fig. S19**. Even though such a figure does not consider the spatial correlation of PE at the grid level, it provides another lens to examine/compare the distribution of PE (and zonation) for all the experiments and their relation to the gridded products.
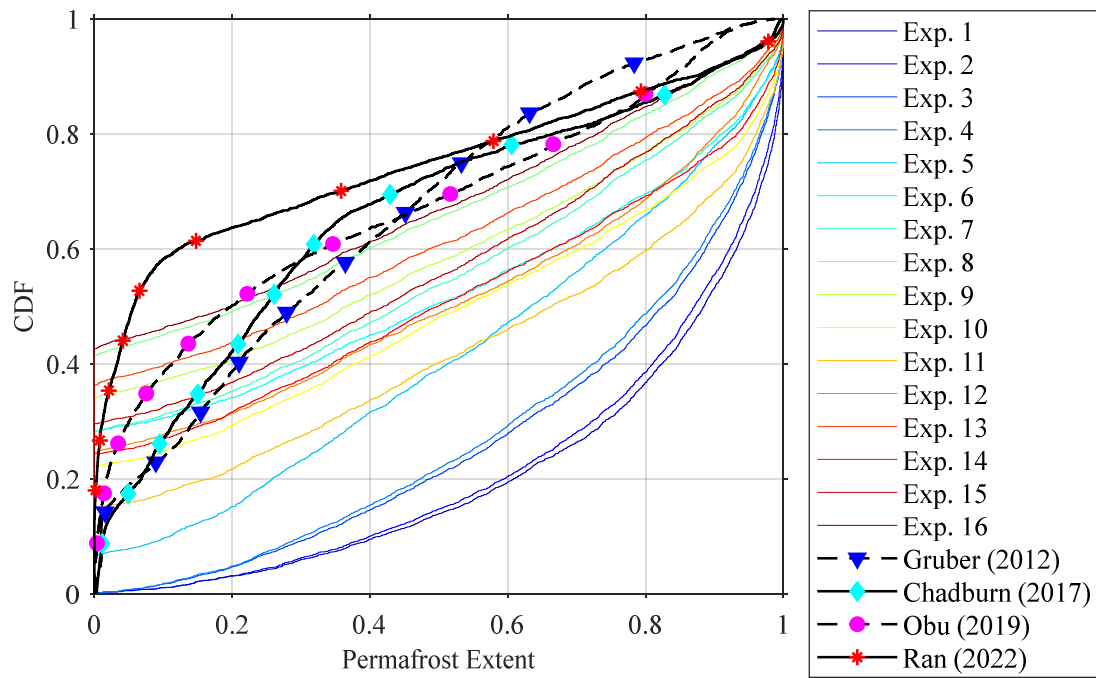
Fig. S19. Cumulative frequency distributions (CDFs) for the simulated and observed permafrost extent averaged over time (2000-2016) and space (LRB domain).

S5.3. Active layer thickness

Similar to **Fig. S19**, the CDFs of the ALT are summarized in **Fig. S20**, which highlights the similarity among the employed datasets in terms of the distribution and the minimum/maximum values. The simulated ALT values were averaged per grid based on the fractional coverage of its GRUs. The figure shows that the model simulations cover a much larger range of ALT than the two considered datasets.
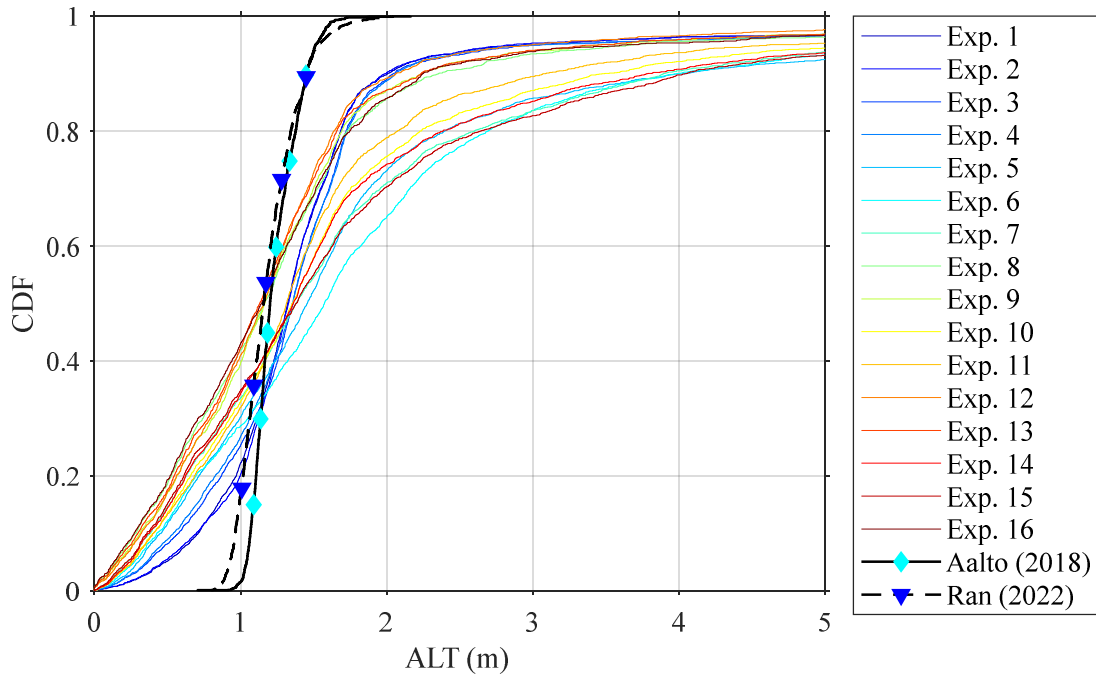
Fig. S20. Cumulative frequency distributions (CDFs) for the simulated and observed Active layer thickness averaged over time (2000-2016) and space (LRB domain).

S5.4. Statistical summary for permafrost gridded products

A summary of Spearman's Rho, the difference (or error), and RMSE for the simulated PE and ALT of all experiments is available in **Table S15**.

Table S15. Summary of comparison metrics of all model experiments (*i.e.* Spearman's Rho, Difference '*or error/bias*', and RMSE) for the simulated permafrost extent and active layer thickness against different gridded products for the 2000-2016 period. Refer to **Table 3** (in the main document) for further information about the configured experiments.

Exp. Id	Permafrost Extent												Active layer thickness					
	Gruber (2012)			Chadburn (2017)			Obu (2019)			Ran (2022)			Aalto (2018)			Ran (2022)		
	Rho	Diff	RMSE	Rho	Diff	RMSE	Rho	Diff	RMSE	Rho	Diff	RMSE	Rho	Diff	RMSE	Rho	Diff	RMSE
1	0.00	0.48	1.04	0.13	0.47	1.03	0.09	0.47	1.06	-0.02	0.59	1.38	-0.04	0.73	2.61	-0.06	0.61	2.40
2	0.01	0.46	1.02	0.13	0.46	1.01	0.06	0.46	1.05	-0.03	0.58	1.37	-0.04	0.71	2.62	-0.06	0.60	2.40
3	0.10	0.42	0.96	0.21	0.41	0.95	-0.02	0.41	1.01	0.03	0.53	1.29	0.00	0.72	2.62	-0.08	0.61	2.43
4	0.12	0.41	0.94	0.23	0.40	0.94	-0.05	0.40	1.00	0.04	0.52	1.28	-0.04	0.70	2.60	-0.09	0.61	2.42
5	0.22	0.29	0.80	0.30	0.28	0.80	0.06	0.26	0.86	0.17	0.36	1.09	-0.05	0.71	2.75	-0.09	0.65	2.57
6	0.45	0.19	0.72	0.56	0.18	0.69	0.18	0.15	0.81	0.47	0.24	0.96	-0.10	0.75	2.73	-0.17	0.62	2.57
7	0.47	0.15	0.67	0.57	0.15	0.64	0.12	0.12	0.80	0.47	0.21	0.91	-0.13	0.68	2.74	-0.22	0.56	2.58
8	0.55	0.03	0.58	0.66	0.02	0.53	0.21	0.01	0.75	0.58	0.09	0.77	-0.40	-0.03	1.53	-0.43	-0.15	1.47
9	0.44	0.09	0.65	0.57	0.09	0.60	0.28	0.08	0.74	0.50	0.17	0.87	-0.41	0.04	1.61	-0.47	-0.08	1.53
10	0.34	0.22	0.76	0.47	0.22	0.74	0.26	0.19	0.79	0.40	0.28	1.02	-0.13	0.66	2.70	-0.22	0.55	2.51
11	0.14	0.29	0.87	0.29	0.28	0.84	0.28	0.26	0.83	0.24	0.36	1.13	-0.13	0.68	2.66	-0.23	0.57	2.49
12	0.18	0.17	0.77	0.36	0.17	0.72	0.31	0.17	0.77	0.28	0.26	1.01	-0.42	0.09	1.78	-0.48	-0.05	1.67
13	0.42	0.07	0.65	0.55	0.06	0.60	0.31	0.06	0.72	0.49	0.14	0.86	-0.40	-0.02	1.60	-0.44	-0.14	1.54
14	0.32	0.20	0.76	0.44	0.19	0.73	0.26	0.17	0.77	0.39	0.26	1.01	-0.13	0.68	2.75	-0.21	0.56	2.59
15	0.46	0.14	0.66	0.57	0.13	0.64	0.12	0.11	0.80	0.47	0.19	0.89	-0.13	0.68	2.75	-0.21	0.56	2.60
16	0.55	0.01	0.57	0.66	0.01	0.52	0.21	0.00	0.75	0.58	0.08	0.76	-0.40	-0.06	1.50	-0.41	-0.18	1.49

S6. Hydrologic assessment

Fig. S21 shows the band of variability across all experiments for the long-term daily mean streamflow for the 2000-2016 period at four gauge stations; performance metrics for each station and experiment are provided in **Table S16**. Interestingly, the PBias decrease as we move downstream the LRB, on average, from -24% at the headwater, to -15% at the outlet; similarly the values of NSE_{Log} and KGE improve toward the basin's outlet. The four hydrographs (**Fig. S21A-D**) highlight the ability of most configurations to correctly predict the peak timing, with a tendency to overestimate its value. Further, the falling limb's slope of each observed hydrograph tends to be overestimated by all model configurations (steeper slope and lower volume), which led to the underestimation of the total volume, as shown by the negative PBias (**Table S16**).
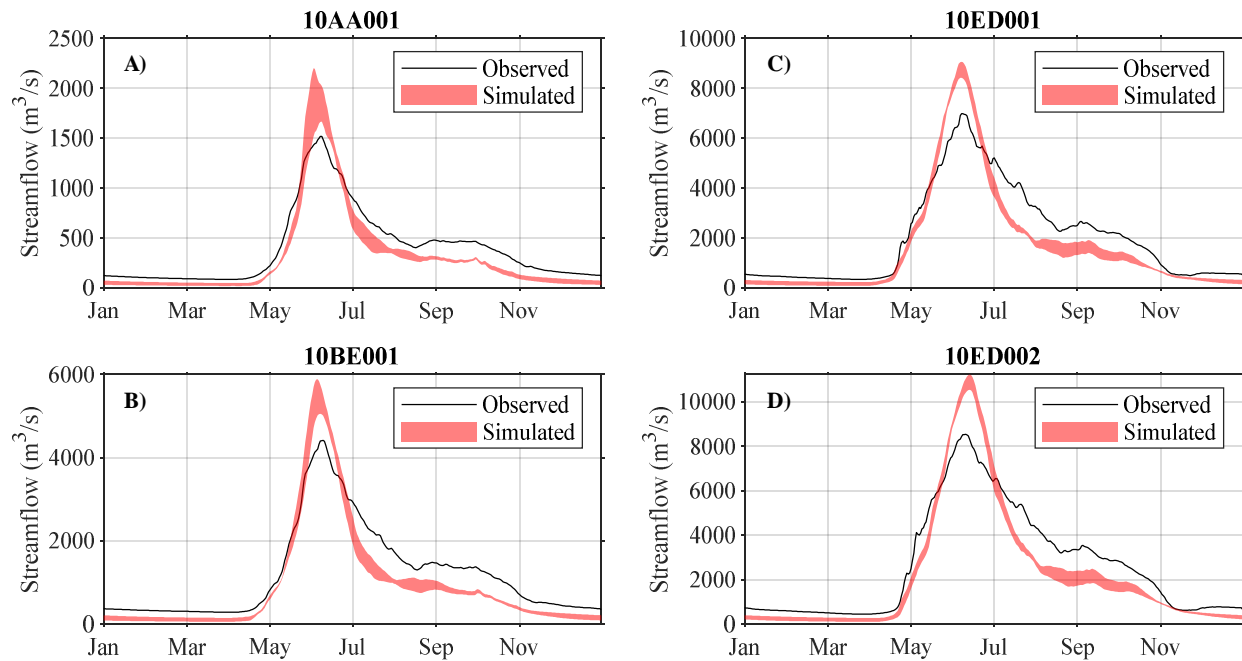
Fig. S21. Long-term mean daily streamflow for the 2000-2016 period (*i.e.,* observed and the variability band across model experiments) at four different gauge stations in the LRB: A) 10AA001 (Headwater), B) 10BE001 (Intermediate), C) 10ED001 (Intermediate), and D) 10ED002 (LRB outlet).

Table S16. Summary of performance metrics for the simulated streamflow of all model experiments at different gauge stations for the 2000-2016 period. Refer to **Table 3** (in the main document) for further information about the configured experiments.

Exp. Id	Headwater (10AA001)				Intermediate (10BE001)				Intermediate (10ED001)				Outlet (10ED002)			
	NSE	NSE_{Log}	KGE	PBias	NSE	NSE_{Log}	KGE	PBias	NSE	NSE_{Log}	KGE	PBias	NSE	NSE_{Log}	KGE	PBias
1	0.63	-0.21	0.65	-22.0	0.69	-0.15	0.70	-22.4	0.73	0.49	0.78	-17.2	0.72	0.46	0.78	-15.9
2	0.62	-0.53	0.63	-22.1	0.68	-0.56	0.69	-22.5	0.73	0.19	0.78	-17.1	0.72	0.19	0.78	-15.7
3	0.62	-0.44	0.63	-22.1	0.68	-0.51	0.69	-22.5	0.73	0.25	0.77	-17.2	0.72	0.25	0.78	-15.7
4	0.62	-0.42	0.63	-22.0	0.68	-0.50	0.69	-22.5	0.73	0.27	0.78	-17.2	0.72	0.27	0.78	-15.8
5	0.70	0.05	0.72	-21.9	0.72	-0.02	0.72	-22.4	0.71	0.48	0.76	-18.8	0.70	0.47	0.76	-17.4
6	0.74	0.42	0.74	-24.0	0.74	0.27	0.73	-24.6	0.68	0.60	0.75	-19.3	0.66	0.59	0.75	-17.8
7	0.73	0.44	0.73	-24.1	0.73	0.27	0.72	-24.6	0.67	0.60	0.74	-19.2	0.65	0.59	0.74	-17.7
8	0.73	0.52	0.75	-22.2	0.74	0.42	0.74	-22.2	0.68	0.64	0.75	-18.0	0.65	0.62	0.74	-16.6
9	0.73	0.45	0.75	-22.2	0.74	0.39	0.74	-22.2	0.68	0.62	0.75	-17.8	0.65	0.59	0.74	-16.3
10	0.73	0.34	0.73	-24.4	0.73	0.19	0.72	-24.8	0.67	0.55	0.74	-19.4	0.65	0.52	0.74	-17.8
11	0.74	0.58	0.75	-23.2	0.75	0.52	0.75	-23.3	0.72	0.76	0.78	-17.3	0.71	0.73	0.78	-16.0
12	0.75	0.64	0.76	-21.9	0.76	0.61	0.76	-21.9	0.73	0.79	0.79	-16.3	0.71	0.77	0.79	-15.0
13	0.73	0.55	0.75	-22.2	0.74	0.43	0.74	-22.3	0.67	0.63	0.74	-17.8	0.65	0.61	0.74	-16.3
14	0.73	0.47	0.73	-23.9	0.73	0.29	0.72	-24.4	0.67	0.58	0.74	-19.2	0.65	0.56	0.74	-17.6
15	0.73	0.48	0.73	-23.9	0.73	0.30	0.72	-24.4	0.67	0.61	0.74	-19.1	0.65	0.60	0.74	-17.7
16	0.73	0.56	0.75	-22.2	0.74	0.44	0.74	-22.3	0.67	0.65	0.75	-18.0	0.65	0.63	0.74	-16.6

Lastly, we examined the variability in water balance partitioning across all H-LSM parameterizations. **Fig. S22A-C** shows the band of variability for the basin's average cumulative evapotranspiration, total runoff, and the change in soil storage, represented by the water equivalent depth (mm). The perturbations made on the LRB H-LSM setup had little effect on the partitioning of surface fluxes (ET and total runoff), as shown by the narrow band of variability across the experiments. However, there is a tangible impact on the basin storage, or to be more specific, the partitioning of ice/liquid water content as shown in **Fig. S22D-F**. Such impact is in line with the changes occurring in the thermal regime, represented by the changes in the soil temperature.
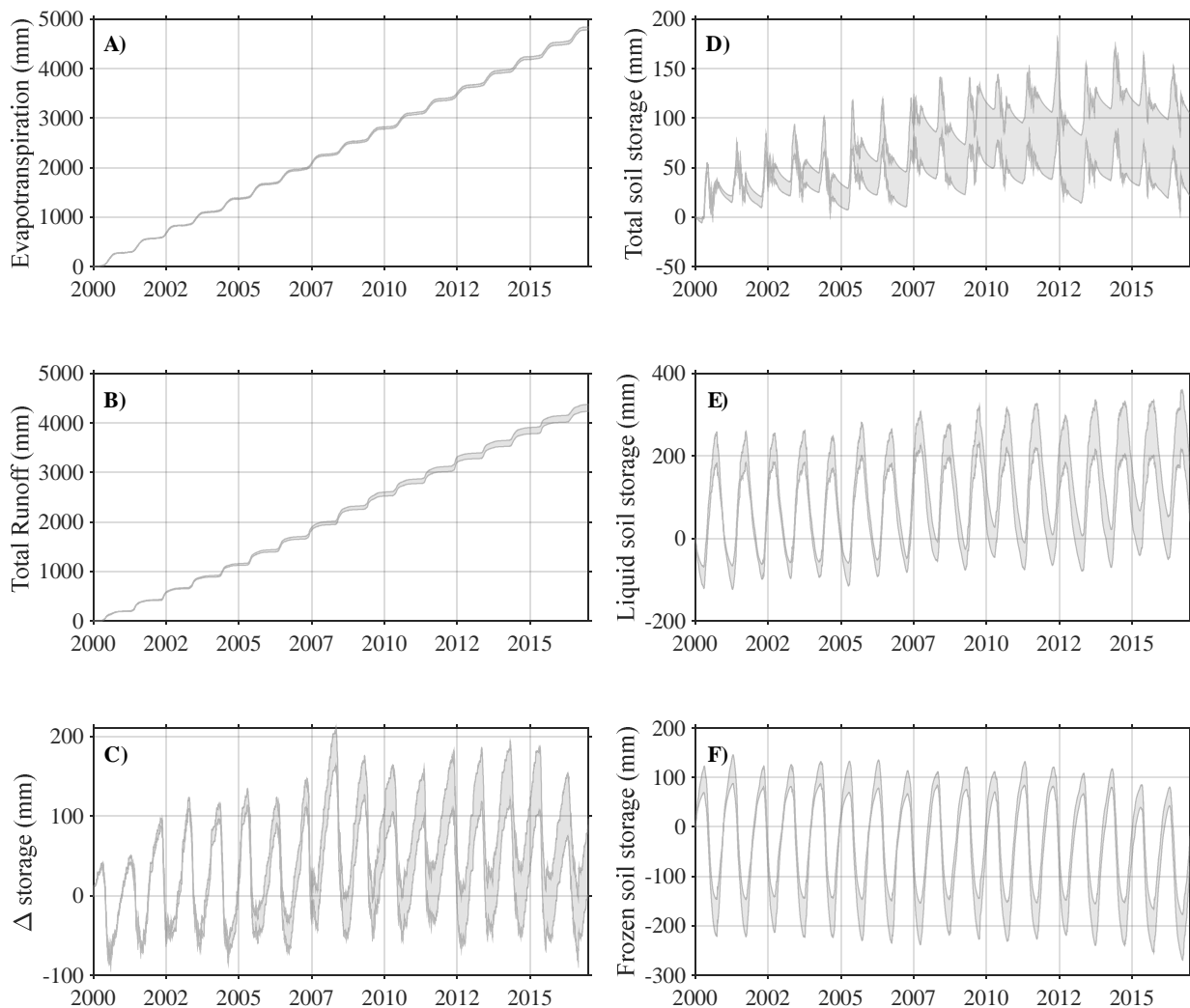
Fig. S22. The band of variability for the partitioning of water-balance components for all model configurations into A) cumulative evapotranspiration, B) total runoff, C) the change in total storage (including soil, canopy, ponding, and snow), D) the change in soil water storage partitioned into E) liquid

soil water and F) frozen soil water. The provided water equivalent depths (mm) correspond to the basin average at a daily time-step.

S7. Experiments overall ranking

Table S17 provides the average ranking of all experiments based on the small-scale assessment of permafrost (ground observations), the large-scale assessment of permafrost (gridded permafrost datasets), and streamflow.

Table S17. Experiments ranking based on their performance against permafrost ground observations, permafrost gridded products, and streamflow. For each criterion, the ranking is averaged over all its items (*i.e.* sites, products, and gauge stations).

Exp. Id	Ground Permafrost Observations	Gridded Permafrost Products	Streamflow
1	8.1	12.9	8.1
2	7.2	12.3	10.0
3	10.3	12.2	10.1
4	11.3	11.4	9.3
5	10.2	11.4	9.7
6	9.9	8.7	9.3
7	11.0	7.7	11.3
8	15.0	3.6	6.3
9	10.1	5.1	6.5
10	3.9	8.9	12.4
11	6.3	10.3	4.3
12	10.5	8.3	1.5
13	10.1	4.6	7.4
14	3.9	8.8	11.7
15	13.4	7.2	10.9
16	15.8	2.7	7.4

S8. References

Burke, E. J., Zhang, Y. and Krinner, G.: Evaluating permafrost physics in the Coupled Model Intercomparison Project 6 (CMIP6) models and their sensitivity to climate change, Cryosph., 14(9), 3155–3174, doi:10.5194/tc-14-3155-2020, 2020.

Canada Centre for Remote Sensing (CCRS), Nacional para el Conocimiento y Uso de la Biodiversidad (CONABIO), Comisión Nacional Forestal (CONAFOR), Insituto Nacional de Estadística y Geografía (INEGI), and U.S. Geological Survey (USGS): 2005 North American Land Cover at 250m spatial resolution, available at: http://www.cec.org/tools-and-resources/map-files/ land-cover-2005 (last access: 15 January 2020), 2010.

Centre for Land and Biological Resources Research. Soil landscapes of Canada (Vol. v.2.2). Canada, 1996.

Chadburn, S. E., Burke, E. J., Cox, P. M., Friedlingstein, P., Hugelius, G. and Westermann, S.: An observation-based constraint on permafrost loss as a function of global warming, Nat. Clim. Chang., 7(5), 340–344, doi:10.1038/nclimate3262, 2017.

Elshamy, M., Princz, D., Sapriza-Azuri, G., Abdelhamed, M. S., Pietroniro, A., Wheater, H. S. and Razavi, S.: On the configuration and initialization of a large-scale hydrological land surface model to represent permafrost, Hydrol. Earth Syst. Sci., 24(1), 349–379, doi:10.5194/hess-24-349-2020, 2020.

Gill, A. E.: Atmosphere - Ocean Dynamics., edited by W. L. Donn, Academic Press, San Diego, California., 1982.

Gruber, S.: Derivation and analysis of a high-resolution estimate of global permafrost zonation, Cryosphere, 6(1), 221–233, doi:10.5194/tc-6-221-2012, 2012.

Harvey, R. and Verseghy, D. L.: The reliability of single precision computations in the simulation of deep soil heat diffusion in a land surface model, Clim. Dyn., 46(11–12), 3865–3882, doi:10.1007/s00382-015-2809-5, 2016.

Ji, H., Nan, Z., Hu, J., Zhao, Y. and Zhang, Y.: On the Spin-Up Strategy for Spatial Modeling of Permafrost Dynamics: A Case Study on the Qinghai-Tibet Plateau, J. Adv. Model. Earth Syst., 14(3), doi:10.1029/2021ms002750, 2022.

Melton, J. R., Verseghy, D. L., Sospedra-Alfonso, R. and Gruber, S.: Improving permafrost physics in the coupled Canadian Land Surface Scheme (v.3.6.2) and Canadian Terrestrial Ecosystem Model (v.2.1) (CLASS-CTEM), Geosci. Model Dev., 12(10), 4443–4467, doi:10.5194/gmd-12-4443-2019, 2019.

Obu, J., Westermann, S., Bartsch, A., Berdnikov, N., Christiansen, H. H., Dashtseren, A., Delaloye, R., Elberling, B., Etzelmüller, B., Kholodov, A., Khomutov, A., Kääb, A., Leibman, M. O., Lewkowicz, A. G., Panda, S. K., Romanovsky, V., Way, R. G., Westergaard-Nielsen, A., Wu, T., Yamkhin, J. and Zou, D.: Northern Hemisphere permafrost map based on TTOP modelling for 2000–2016 at 1 km2 scale, Earth-Science Rev., 193(March), 299–316, doi:10.1016/j.earscirev.2019.04.023, 2019.

Ran, Y., Li, X., Cheng, G., Che, J., Aalto, J., Karjalainen, O., Hjort, J., Luoto, M., Jin, H., Obu, J., Hori, M., Yu, Q. and Chang, X.: New high-resolution estimates of the permafrost thermal state and hydrothermal conditions over the Northern Hemisphere, Earth Syst. Sci. Data, 14(2), 865–884, doi:10.5194/essd-14-865-2022, 2022.